

Article

Nonlinear Vibrations of Innovative One-Way Clutch in Vehicle Alternator

Xiaotian Xu ¹ , Gang Chen ^{1,*}, Joshua Colley ¹, Pengrui Li ¹ and Mohamad Qatu ²

¹ College of IT & Engineering, Marshall University, Huntington, WV 25755, USA; xu33@marshall.edu (X.X.); cooley_2007@hotmail.com (J.C.); li75@live.marshall.edu (P.L.)

² College of Technology, Eastern Michigan University, Ypsilanti, MI 48197, USA; mqatu@emich.edu

* Correspondence: chenga@marshall.edu; Tel.: +1-304-634-8138

Received: 27 May 2018; Accepted: 26 July 2018; Published: 30 July 2018



Abstract: One-way clutches have been proposed for vehicle alternators. The clutch can play an important role in reducing vibrations of the vehicle engine accessory system, but the severe vibrations of the clutch subsystem limit its stability and durability. This paper investigates the nonlinear vibrations of a one-way clutch between the accessory pulley and the alternator shaft. The one-way clutch is modelled as a discontinuous stiffness system, and the simplified model is analyzed using discontinuous transform to determine the periodic, primary resonance and the sub and super harmonic resonance solutions. The typical system model is numerically solved and the spectrum and phase plots are characterized. The results give a big picture of and insights into the nonlinear vibration features of one-way clutch system. A relevant US patent is pending.

Keywords: vehicle alternator; engine system; front-end accessory; belt-pulley system; one-way clutch; nonlinear dynamics

1. Introduction

Vehicle engine front-end accessory drive systems are widely used in passenger vehicles and heavy-duty trucks. Using a single belt, engine power is delivered from the crankshaft to a variety of accessories such as the air conditioner, alternator, power steering, water pump among others. Crankshaft torque pulsations from the cylinder combustion in the engine, and dynamic accessory torques could excite severe rotational vibrations of the subsystems [1–3]. The periodic firing of the engine cylinders causes the crankshaft to have periodic motion superimposed on a steady angular velocity. This periodic motion is transferred to various engine accessories. As the engine speed increases, the frequency of crankshaft pulses increases, causing belt tension drop and belt slip on the pulley. The alternator, with its very large moment of inertia, is most susceptible to dynamic tension fluctuations; hence, there is a need to find ways to reduce the steady-state peak tension drop across it. To address the issues of vibration, one-way clutch pulleys have been developed and used in vehicle alternators [4–9]. With the aim of detaching the alternator from the rest accessory subsystem during high speed transients and to reduce the transmission of torsional vibrations from the internal combustion engine to the engine accessories, one-way clutches have been used more and more frequently to decouple the alternator system and reduce the system's vibrations. The one-way clutches with wrap springs have been introduced into the generator to allow the high inertia element to overrun the system when the pulley is decelerating.

To avoid the impact generated during system engagements, the wrap spring one-way clutch, also called over-running alternator de-coupler (OAD), as shown in Figure 1 was used. It has a torsional wrap spring-damper that connects the pulley to the outer ring of the clutch [4–8]. In wrap-spring

clutches, a helical spring, typically wound with square-cross-section wire, is used. The torsion spring also acts as a dampening mechanism which greatly reduces the belt vibration.

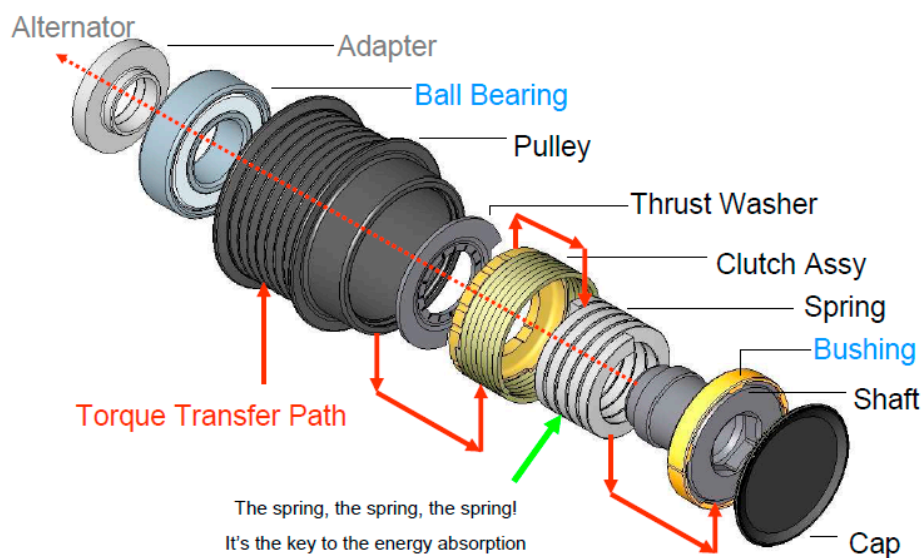


Figure 1. Schematic of one-way clutch alternator pulley.

The application of the one-way clutch has a strong influence on the entire system's dynamic behavior. Under certain circumstances, the unique features of the one-way clutch allow the belt spans to experience large transverse vibrations or the clutch to have larger torsional vibrations. There are many research studies dedicated to the vibration analysis of a one-way clutch. To accurately predict the entire system's dynamic behavior, the motions of the one-way clutch need to be considered in the models. This results in a strong nonlinear system due to the special stiffness discontinuous property of the one-way clutch. Balaji and Mockensturm established a mathematical model of accessory system with seven pulleys with a one-way clutch, and the piece-wise linear system is numerically solved for specific cases using the Runge-Kutta method [10]. Ding and Zu solved a similar model numerically and used fast Fourier transform to derive the natural frequency of the nonlinear vibration [11]. For the similar model, Ding and Hu used two different approaches: (a) The nontrivial solutions of viscoelastic model; and (b) the iterative solution, to determine the nontrivial equilibriums of dynamical system numerically. They also studied the natural frequencies of the system by using the Galerkin method [12]. Zhu and Parker established a model of the accessory system with two pulleys having a one-way clutch, and the dynamical system was analyzed by using the harmonic balance method, with the dynamical properties characterized in terms of spring stiffness, excitation amplitude, and moment inertia of pulleys [13]. Zeng and Shangguan established a model of the accessory system, with three pulleys having a one-way clutch, which consists of a driving pulley, a driven pulley and a tensioner. The dynamical system is analyzed numerically by using the Gear method, with the dynamical properties being characterized and optimized in terms of clutch spring stiffness, excitation amplitude and moment inertia of pulleys [14]. In-vehicle experimental tests are a significant way to investigate the vibrations of alternator pulleys. An experimental procedure, including proper selection of parameters, measures and sensors, to evaluate the potential vibrations of each alternator pulley is proposed by Michelotti, Pastorelli et al. [15]. The existing research characterizes many linear and nonlinear vibration properties of one-way clutch for many specific cases. There has been a lack of overall understanding of global characteristics of the strong nonlinear vibrations of one-way clutch system. For practicing accessory drive designers in the automotive/heavy vehicle industries, the natural frequencies and dynamic response are of utmost interest. Predicting the system's dynamic behavior in the design stage is important because the changes are difficult to accomplish once

prototypes are built. This requires a comprehensive model of the one-way clutch to characterize the system’s properties, particularly all kinds of resonances. In this paper, the functional principles of the one-way clutch will be theoretically investigated and explained while the comprehensive resonance features will be reported. The analytical results clearly show that there exist primary, subharmonic, and superharmonic resonances. The numerical analysis illustrated the detailed cases. This study offers some insights for the product design into how to pinpoint and avoid varied resonance cases.

2. Mathematical Model

Based on the real system of the wrap-spring one-way clutch [4–13], the model is given as follows. When the rotations of the wrap-spring ends, for which the pulley rotation exceeds the accessory shaft rotation, then the clutch is engaged. Power transmission takes place from the driving to the driven pulley. For the alternate case where accessory rotation is less than pulley rotation, the wrap-spring diameter decreases and the clutch disengages; no torque is transmitted. A theoretical model of one-way clutch on a two-pulley system is shown in Figure 2. The driving pulley represents the crankshaft, and its motion is specified as harmonic oscillation. In vehicle applications, engine firing pulsations induce periodic fluctuations in crankshaft speed at the firing frequency. The driven pulley was connected to the accessory. The one-way clutch is integrated between the accessory pulley and the alternator shaft. The mathematical model of the system is given by the following equations:

$$\begin{cases} J_p \ddot{\theta}_p + c_p \dot{\theta}_p + k_p \theta_p + g(\theta_p - \theta_a) = M \cos \omega t \\ J_a \ddot{\theta}_a + c_a \dot{\theta}_a + k_a \theta_a + g(\theta_a - \theta_p) = 0 \end{cases} \tag{1}$$

in which: θ_p and θ_a are the vibration angle of driven pulley and alternator shaft, respectively; J_p and J_a are the moment of inertia of driven pulley and alternator shaft, respectively; c_p and k_p are the damping and stiffness constants associated with driven pulley, respectively; $k_p = 2K_b r_p^2$, and c_a and k_a are the damping and stiffness constants associated with the rotor of alternator, respectively. M and ω are respectively the amplitude and frequency of excitation acted on driven pulley due to engine firing excitation. The torque transmitted between the accessory pulley and alternator shaft is given as follows,

$$g(\theta_p - \theta_a) = \begin{cases} k_d(\theta_p - \theta_a), & \theta_p > \theta_a \\ 0, & \theta_p < \theta_a \end{cases} \tag{2}$$

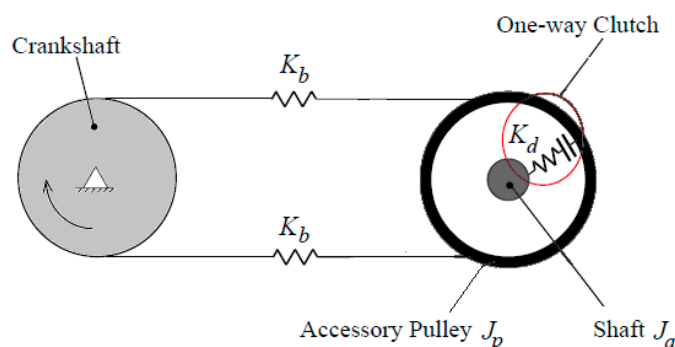


Figure 2. Theoretical model of one-way clutch in accessory system.

The equation described by Equation (1) has been studied numerically and theoretically under particular conditions [13].

Generally, Equation (1) represents a strong nonlinear system. Consider the simplest case, $\theta_p \geq \theta_a$; the system is linear and the squares of the natural frequencies are derived as

$$\omega_{21,22}^2 = \left(\frac{k'_{11}}{J_p} + \frac{k'_{22}}{J_a}\right)/2 \mp \sqrt{\left(\left(\frac{k'_{11}}{J_p} + \frac{k'_{22}}{J_a}\right)^2 - 4\left(\frac{k'_{11}k'_{22}}{J_p J_a} - \frac{k'_{12}k'_{21}}{J_p J_a}\right)\right)}/2} \tag{3}$$

in which $k'_{11} = k_p + k_d$, $k'_{12} = k_d = k'_{21}$ and $k'_{22} = k_a + k_d$. Furthermore, letting $k_d = 0$, which deteriorates to the natural frequencies of two independent systems: The accessory system and the uncoupled alternator. For the case with both $\theta_p \geq \theta_a$ and $\theta_p \leq \theta_a$, the system exhibits a nonlinear feature.

Consider the case in which the driven pulley mode and alternator shaft mode motion can be decoupled, and we just discuss driven pulley mode, then Equation (1) can be approximated by

$$\begin{aligned} J_p \ddot{\theta}_p + c_p \dot{\theta}_p + k_p \theta_p + k_d(\theta_p - \theta_a) &= M \cos \omega t, & \theta_p \geq \theta_a \\ J_p \ddot{\theta}_p + c_p \dot{\theta}_p + k_p \theta_p &= M \cos \omega t, & \theta_p \leq \theta_a \end{aligned} \tag{4}$$

By using the approach given in References [16,17], a comprehensive analytical solution is systematically derived through the discontinuous transformation, and the results are given in next section.

3. Theoretical Analysis

Closed form analytical solutions are of great significance in configuring the overall vibration characteristics. The problem described by Equation (4) is identical to the harmonic force excited by the unsymmetrical piecewise-linear spring-damping system. Because the non-linearities in this problem cannot be assumed to be small, a general analytical solution, by only using conventional methods such as the perturbation method, is not feasible. By using the discontinuous transformation method [16,17], a far-from resonance solution, nearly a primary resonance solution, a super-harmonic resonance solution and a sub-harmonic resonance solution are systematically derived as follows:

3.1. Free Vibration (under Unit Initial Condition)

$$\begin{aligned} \theta_p = \frac{\omega_0}{2\omega_1} \cos \omega_1 t + \left(1 - \frac{\omega_0}{2\omega_1}\right) \cos(\omega_2 t - \beta_0) + \frac{1}{\pi} \sum_{n=1}^{\infty} \frac{\sin n\alpha_0 \cos(\omega_1 + n\omega_0)t + \cos(\omega_1 - n\omega_0)t}{n} \\ - \frac{\omega_1}{\pi\omega_2} \sum_{n=1}^{\infty} \frac{\sin n\alpha_0 \cos[(\omega_1 + n\omega_0)t + \beta_0] + \cos[(\omega_2 - n\omega_0)t + \beta_0]}{n} \end{aligned} \tag{5}$$

in which $\omega_1 = \sqrt{k_p/J_p}$, $\omega_2 = \sqrt{(k_p + k_d)/J_p}$, $\omega_0 = 2\omega_1\omega_2/(\omega_1 + \omega_2)$, $\alpha_0 = \pi\omega_0/(2\omega_1)$, $\beta_0 = \pi(1 - \omega_2/\omega_1)/2$.

3.2. Far-From Resonance Solutions

$$\begin{aligned} \theta_p = \frac{M(\omega_2^2 - \omega_1^2)}{\pi J_p (\omega_1^2 - \omega^2)(\omega_2^2 - \omega^2)} + \frac{M(\omega_1^2 + \omega_2^2 - 2\omega^2)}{2J_p (\omega_1^2 - \omega^2)(\omega_2^2 - \omega^2)} \sin \omega t \\ + \frac{2F(\omega_2^2 - \omega_1^2)}{\pi J_p (\omega_1^2 - \omega^2)(\omega_2^2 - \omega^2)} \sum_{n=1}^{\infty} \frac{\cos 2n\omega t}{(2n + 1)(2n - 1)} \\ + \frac{1}{2} [A_1 \sin \omega_1 t + A_2 \sin(\omega_2 t + \beta_0)] \\ + \frac{A_1}{\pi} \sum_{n=1,3,5}^{\infty} \frac{\cos(\omega_1 - n\omega)t - \cos(\omega_1 + n\omega)t}{n} \\ - \frac{A_2}{\pi} \sum_{n=1,3,5}^{\infty} \frac{\cos[(\omega_2 - n\omega)t + \beta_0] - \cos[(\omega_1 + n\omega)t + \beta_0]}{n} \end{aligned} \tag{6}$$

in which $\beta_0 = -\pi\omega_2/\omega$, $A_1 = M\omega/[J_p\omega_1(\omega^2 - \omega_1^2)]$, $A_2 = -M\omega/[J_p\omega_2(\omega^2 - \omega_2^2)]$.

3.3. Near-Primary Resonance Solutions

$$\theta_p = \left[\frac{2M}{(\omega_2^2 - \omega_1^2)J_p(2\Delta + 1)} + \frac{3M}{4\omega^2 J_p(2\Delta + 1)^2} \right] \sin \omega t - \frac{\pi J_p}{2\omega^2 J_p(2\Delta + 1)} \cos \omega t$$

$$+ \frac{M}{\pi\omega^2 J_p(2\Delta + 1)} \sum_{n=1,3,5}^{\infty} \frac{\cos(n-1)\omega t - \cos(n+1)\omega t}{n}$$

$$- \frac{M(\omega t - \pi)}{\pi\omega^2 J_p(2\Delta + 1)} \sum_{n=1,3,5}^{\infty} \frac{\sin(n-1)\omega t + \sin(n+1)\omega t}{n}$$
(7)

where $\Delta = (\omega_1^2 - \omega^2) / (\omega_2^2 - \omega_1^2)$.

3.4. Super-Harmonic Resonance Solutions

$$\theta_p = \frac{M(2n^2\omega^2 - \omega^2 - \omega_1^2)}{J_p(n^2 - 1)^2\omega^4} \sin \omega t + \frac{2M((\omega_2^2 - \omega_1^2))}{\pi J_p(n^2 - 1)^2(\omega_1^2 - n^2\omega^2)\omega^2} \cos \omega t$$

$$- \frac{2M((\omega_2^2 - \omega_1^2))}{\pi J_p(n^2 - 1)^2(\omega_1^2 - n^2\omega^2)\omega^2} \cos n\omega t, \quad n = 2, 3, 4, \dots$$
(8)

3.5. Sub-Harmonic Resonance Solutions

For the case of $\omega_2 \gg \omega_1$, it can be derived out that the approximate solution in the proximity of sub-harmonic resonant frequency is:

$$\theta_p = \frac{4lM}{\pi^2 J_p \omega_1 (l^2 - 1) (\omega - l\omega_1)} \sum_{n=1,3,5}^{\infty} \frac{\cos \left[\frac{(n+1)\omega t}{l} \right] - \cos \left[\frac{(n-1)\omega t}{l} \right]}{n}, \quad l = 2, 4, 6, \dots$$
(9)

Figure 3 illustrates a typical result of the response amplitude as a function of the excitation frequency ratio. The curve in Figure 3 exhibits a series of resonant peaks including the 1/2th and 1/3th order superharmonic resonance, 2nd and 3rd order subharmonic resonance as well as the primary resonance. It is noted that in existing research, certain experiments [9,15,18] were conducted and compared with preceding linear vibration theory of a one-way spring clutch. This paper proposed an advanced nonlinear vibration theory of the one-way clutch which encompasses the linear cases, and as such, it is consistent with all existing experimental results.

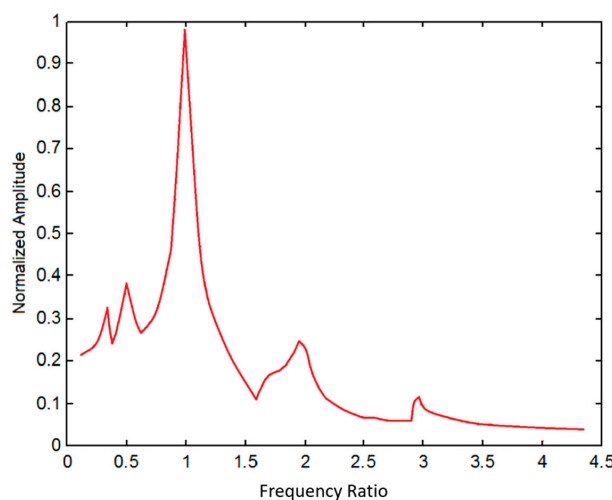


Figure 3. The frequency response function ($\frac{k_d}{k_p} = 4, \zeta = 0.05$).

4. Numerical Analysis

In this section, the numerical analysis of a typical one-way clutch system, characterized by Equation (1), is presented. Table 1 shows the parameters for the typical system. The frequency, ω_0 , is considered as the natural frequency for the linear single degree of freedom system when the accessory is not equipped with one-way clutch, and $\omega_0 = \sqrt{k_p / (J_p + J_a)}$. Corresponding to the case of the linear system which is mentioned in Section 2, the dimensionless natural frequencies are $\Omega_1 = \omega_1 / \omega_0 = 0.987$ and $\Omega_2 = \omega_2 / \omega_0 = 6.931$ for the values in Table 1. These two dimensionless natural frequencies could be the criterion to evaluate how the system works under different conditions.

Table 1. Parameters for typical cases.

| | |
|---------------------------------|----------------------------|
| Radius of Driven Pulley | 0.0286 (m) |
| Radius of crankshaft | 0.04 m |
| Driven Pulley Moment of Inertia | 0.0016 (kgm ²) |
| Alternator Moment of Inertia | 0.0050 (kgm ²) |
| Modal damping ratio | 5% |
| Belt stiffness | 250 kN/m |
| Clutch spring stiffness | 50–1500 Nm/rad |
| Excitation amplitude | 0.001 rad |
| Preload | 2.3 Nm |

To conduct the numerical analysis of the dynamic model with the above parameters using MATLAB, the discontinuous stiffness nonlinearity which was indicated by Equation (2) can be efficiently approximated as a continuous function. A smoothed function is used to approximate the discontinuous stiffness nonlinearity $g(\theta_p - \theta_a)$.

$$g(\delta\theta) = \frac{1}{2}K_d[1 + \tanh(\varepsilon\delta\theta)]\delta\theta \tag{10}$$

in which $\delta\theta = \theta_p - \theta_a$, and the ε is the smooth constant which is usually a large positive number, for instance, $\varepsilon = 10,000$ [13]. The clutch torque is approximated by a hyperbolic tangent function as shown in Figure 4. What we want the approximated function to be is a proportional function, with the slope being K_d when $\delta\theta \geq 0$ and being 0 when $\delta\theta \leq 0$. As shown by the results in Figure 4, the approximation is obviously not accurate when $\varepsilon = 10$ because the curve deviates from the desired trajectory, and the satisfied approximation is likely to be obtained for large $\varepsilon > 100$. This is because the results of $\varepsilon = 100$ and $\varepsilon = 10,000$ look to have overlapped each other in the figure. The actual effects of different values of ε will be further investigated when conducting the frequency analysis by employing these values below.

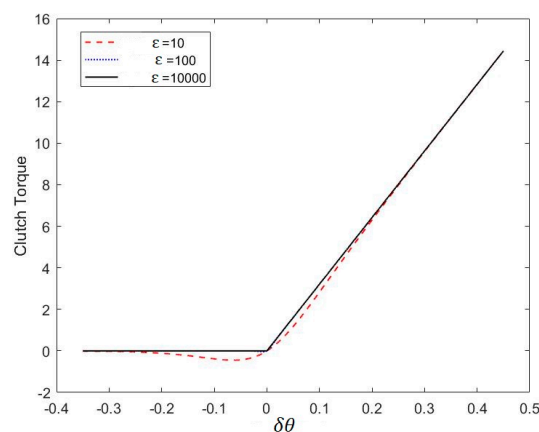


Figure 4. The clutch torque (smooth function) with different smooth constants.

From numerical investigation, we can estimate the effects of the approximations with a different smooth constant, ϵ , for frequency analysis of the system as shown in Figure 5. In this case, Ω is the ratio of excitation frequency and natural frequency of the system.

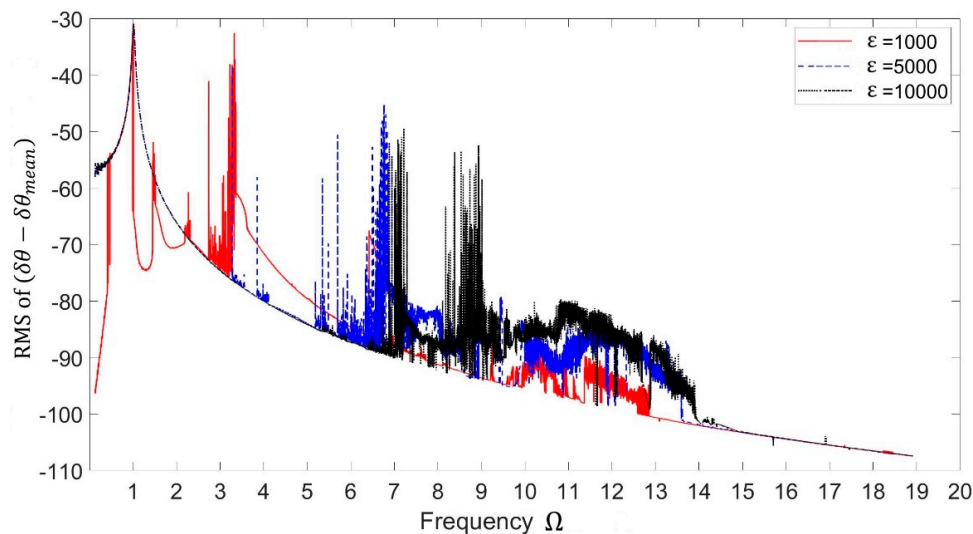


Figure 5. The frequency responses with different values of ϵ .

From investigation we found that the approximation is compromised in numerical analysis with $\epsilon = 1000$ because the trajectory is not only discontinuous and disorderly, but also violate the natural frequencies we derived above. An acceptable approximation is attained by using $\epsilon = 5000$. The approximation is well accomplished by using $\epsilon = 10,000$, the curve is continuous, and we can clearly see the peaks of resonance around Ω_1 and Ω_2 . Thus, a value $\epsilon > 10,000$ is employed when conducting the following numerical analysis.

In the engine front-end accessory system, the excitation frequency is the engine firing frequency which changes in a wide range. The root mean square (r.m.s.) of dynamic amplitude of the relative pulley-accessory rotation, $\delta\theta - \delta\theta_{mean}$, versus excitation frequency, for different values of damping ratios ($\xi = 3\%$, 5% and 8%), are calculated and the results are shown in Figure 6 for the parameters listed in Table 1.

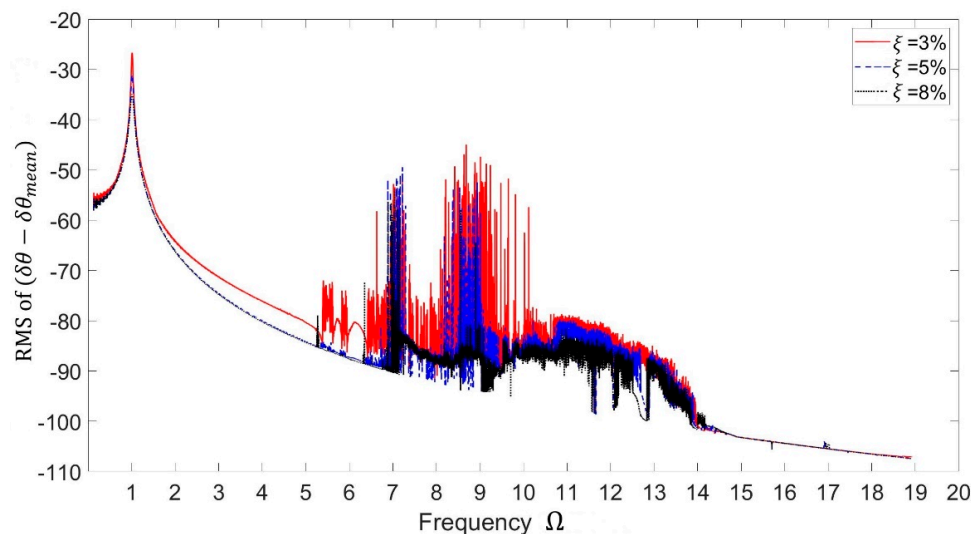


Figure 6. The frequency responses with different damping ratios.

The frequency response for $\zeta = 8\%$ shows that the behavior can be considered as linear. For $\zeta = 3\%$ and 5% , non-linear phenomena appear. It indicates that the system is sensitive to the excitation amplitude. As we can see, there are two resonant regions within the two natural frequencies. The system is linear when the clutch is engaged. The non-linearity occurs near the second resonant region due to the decoupling of the clutch where the spring between pulley and accessory shaft is inactive. The pulley and accessory shaft rotate in opposite directions near the second resonant region. This behavior is called out-of-phase motion, and it tends to clutch disengagement. The amplitude is higher near the first resonant region because of the in-phase motion of pulley and accessory shaft. This means that the pulley and accessory shaft move in the same direction and are excited more directly by the excitation from crankshaft vibration.

In this section, we employ a hyperbolic tangent function to approximate the discontinuous nonlinearity of the system when conducting numerical analysis. Actual effects of different parameters, smooth constant ε and damping ratio ζ , on the numerical analysis of the mathematical model are investigated.

The phase plot and time response are shown in Figures 7 and 8, respectively, by employing a sample excitation frequency of $\omega = 150$ rad/s. The relative displacement $\delta\theta$, which is $\theta_p - \theta_a$, was considered as an important value to investigate the response of the dynamic system.

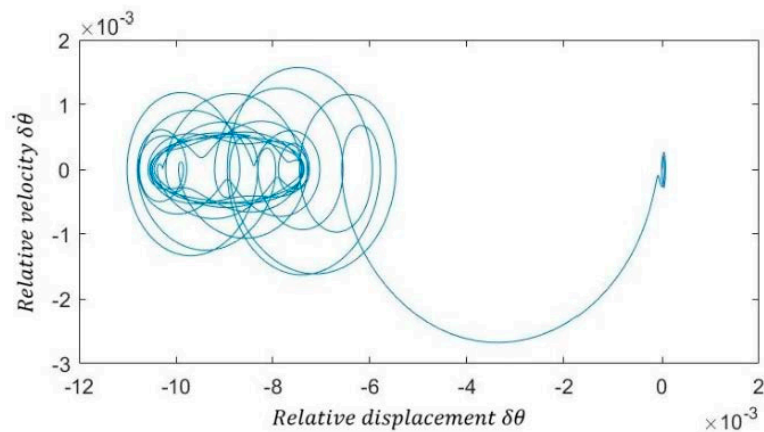


Figure 7. Phase plot: velocity, $\delta\dot{\theta}$, vs. displacement, $\delta\theta$.

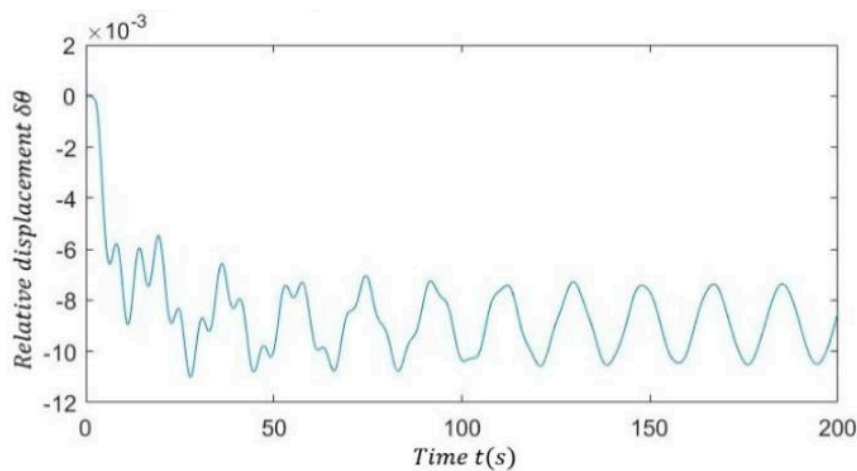


Figure 8. Time response of $\delta\theta$.

The corresponding periodogram power spectral density estimate of $\delta\theta$ and waterfall plot of the spectra of $\delta\theta$ are shown in Figures 9 and 10.

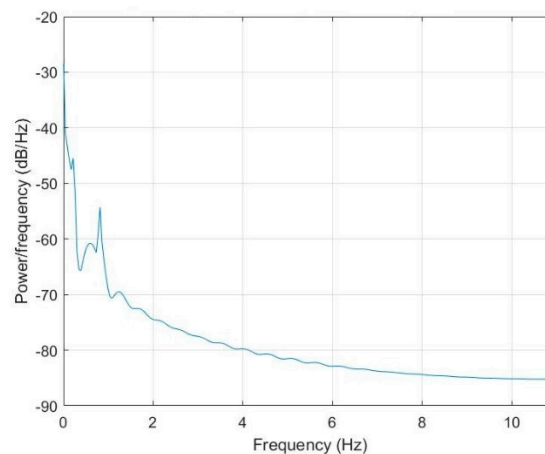


Figure 9. Periodogram power spectral density of $\delta\theta$.

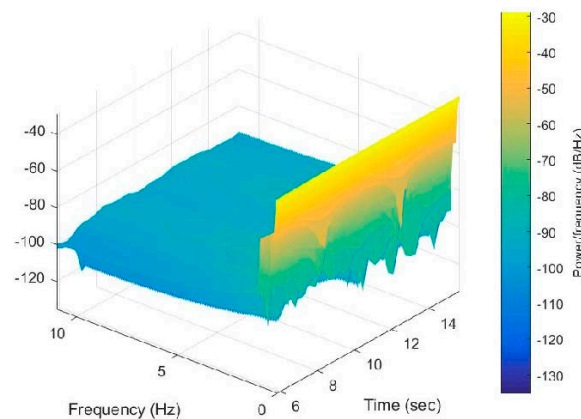


Figure 10. Waterfall spectrum.

5. Conclusions

In this work, nonlinear vibrations of one-way clutch in vehicle alternator system were modeled and analyzed. A special attention was paid to comprehensive resonance properties of the nonlinear system with bilinear stiffness non-smooth features. A two degrees-of-freedom lumped parameters model was employed to account for torsional vibrations of the accessory system with one-way clutch and the model was then simplified as a one degree-of-freedom system so as to derive a comprehensive closed form solution. A non-smooth transformation was used to analyze the simplified model and derive the solution. Our theoretical analysis has shown that the mathematical model is capable of predicting a full range of dynamic responses properties including the primary, subharmonic and superharmonic resonances. Numerical analysis was conducted for the two degrees-of-freedom lumped parameters model, which pinpointed the true dominant nonlinear vibration modes. A global analysis showed different scenarios that allowed an in-depth and general understanding of the one-way clutch dynamics to be developed, whereas the numerical analysis helped to elaborate the detailed vibration patterns related to specific parameters and define critical behaviors of the system. It is noted that conventionally modeling and analyzing of torsional vibrations of engine front-end accessory drive system have treated real global system to be a multiple degree-of-freedom system with sufficient accuracy. As such, the lumped parameter system model used in this paper is accurate enough for the application of alternator clutch subsystem.

Author Contributions: Conceptualization, G.C. and M.Q.; Methodology, G.C.; Software, X.X.; Validation, J.C., P.L.; Formal Analysis, G.C., X. X.; Investigation, J.C., P. L., X.X.

Funding: This research was funded by ALT America INC grant number MURC216132.

Conflicts of Interest: The authors declare no conflict of interest.

References

1. Abrate, S. Vibrations of belts and belt drives. *Mech. Mach. Theory* **1992**, *27*, 645–659. [CrossRef]
2. Beikmann, R.S.; Perkins, N.C.; Ulsoy, A.G. Design and analysis of automotive serpentine belt drive systems for steady-state performance. *ASME J. Mech. Des.* **1997**, *119*, 162–168. [CrossRef]
3. Sheng, G.; Liu, K.; Otramba, J.; Pang, J.; Dukkupati, R.V.; Oatu, M. Model and experimental investigation of belt noise in automotive accessory belt drive. *Int. J. Veh. Noise Vib.* **2004**, *1*, 68–82. [CrossRef]
4. King, R.; Monahan, R. Alternator pulley with integral overrunning clutch for reduction of belt noise. *SAE Tech. Pap.* **1999**, 27–32. [CrossRef]
5. Xu, J.; Antchak, J. New technology to improve the performance of front end accessory drive system. *SAE Tech. Pap.* **2004**. [CrossRef]
6. Cooley, J.; Chen, G. One-Way over-Running Alternator Clutch. U.S. Patent 5598913A, 7 June 1995.
7. Michelotti, A.; Paza, A.L.; Maurici, A.; Foppa, C.; Drabison, J.S.; Morris, Z.; Monahan, R.E. Functional testing of alternator pulleys in chassis dynamometer. *SAE Tech. Pap.* **2013**. [CrossRef]
8. Michelotti, A.; Paza, A.L.; Maurici, A.; Foppa, C. Future trends in the conceptual design alternator pulleys. *SAE Tech. Pap.* **2012**. [CrossRef]
9. Fitz, F.; Cali, C. Controlled alternator decoupling for reduced noise and vibration. *SAE Tech. Pap.* **2010**. [CrossRef]
10. Balaji, R.; Mockensturm, E.M. Dynamic analysis of a front-end accessory drive with a decoupler/isolator. *Int. J. Veh. Des.* **2005**, *39*, 208–231. [CrossRef]
11. Ding, H.; Zu, J.W. Steady-state responses of pulley-belt systems with a one-way clutch and belt bending stiffness. *J. Vib. Acoust.* **2014**, *136*. [CrossRef]
12. Ding, J.; Hu, Q. Equilibria and free vibration of a two-pulley belt-driven system with belt bending stiffness. *Acta Mech.* **2017**, *228*, 3307–3328. [CrossRef]
13. Zhu, F.; Parker, R.G. Non-linear dynamics of a one-way clutch in belt-pulley systems. *J. Sound Vib.* **2005**, *279*, 285–308. [CrossRef]
14. Zeng, X.; Shangguan, W. Modeling and optimization dynamic performances for an engine front end accessory drive system with overrunning alternator decoupler. *Int. J. Veh. Noise Vib.* **2012**, *8*, 261–274. [CrossRef]
15. Michelotti, A.; Pastorelli, P.; Ferreira, A.; Berto, L.; Takemori, C.K. In-vehicle experimental tests to evaluate the performance of alternator pulleys. *SAE Tech. Pap.* **2017**. [CrossRef]
16. Pilipchuk, V.N. Analytical study of vibrating systems with strong non-linearities by employing saw-tooth time transformation. *J. Sound Vib.* **1996**, *192*, 43–64. [CrossRef]
17. Pilipchuk, V.N.; Vakakis, A.F.; Azeez, M.A.F. Study of a class of subharmonic motions using a non-smooth temporal transformation (NSTT). *Phys. D: Nonlinear Phenom.* **1997**, *100*, 145–164. [CrossRef]
18. Pastorelli, P.; Michelotti, A.; Berto, L.; Ferreira, A. Analytical models for spring one-way clutch and torsional vibration dampening systems with experimental correlation. *SAE Tech. Pap.* **2017**. [CrossRef]



© 2018 by the authors. Licensee MDPI, Basel, Switzerland. This article is an open access article distributed under the terms and conditions of the Creative Commons Attribution (CC BY) license (<http://creativecommons.org/licenses/by/4.0/>).